RESEARCH PAPER

Acta Neurobiol Exp 2022, 82: 327–335
DOI: 10.55782/ane-2022-031

Study on the role of immune-related genes after intracranial subarachnoid hemorrhage

Qiaoying Li, Zhong Ren, Dan Fan, Yidan Zhang*

Department of Neurology, Affiliated Hospital of Changchun University of Traditional Chinese Medicine, Changchun, Jilin, China,
** Email: yidanzhang5656@163.com*

We aimed to screen the feature genes related to subarachnoid hemorrhage (SAH). The datasets (GSE73378 and GSE36791) were downloaded from National Center for Biotechnology Information database. Limma package in R was used to screen the differentially expressed genes (DEGs). Single sample gene set enrichment analysis algorithm was used to evaluate the type of immune infiltration. Gene Ontology and Kyoto Encyclopedia of Genes and Genomes (KEGG) pathway analysis were used to analyze function of DEGs. The support vector machine (SVM) was used to constructed classifier, which was evaluated using receiver operating characteristic curves. The E-TABM-421 was used to verify the DEGs related to immunity and the classifier. Seven types of immune cells with significant differences were screened, such as activated CD8 T cell and center memory CD4 T cell. We then obtained 408 DEGs related to immune cell. Subsequently, 10 overlapped KEGG pathways related to the DEGs were obtained, such as hematopoietic cell lineage, NOD-like receptor signaling pathway and T cell receptor signaling pathway. Finally, 9 DEGs related to immune cells (*CCL5*, *CD27*, *CD3D*, *CREB5*, *FYN*, *ITPR3*, *TAB1*, *NCR3* and *S1PR5*) were screened to constructed SVM classifier. The area under the curve was 0.865 in training dataset and the AUC was 0.75 in the validation set. A SVM classifier based on the 9 DEGs (*CCL5*, *CD27*, *CD3D*, *CREB5*, *FYN*, *ITPR3*, *TAB1*, *NCR3* and *S1PR5*) related to immune cells might effectively identify SAH patients or healthy people.

Key words: intracranial subarachnoid hemorrhage, immune-related genes, diagnosis, SVM classifier

INTRODUCTION

Intracranial aneurysms (IAs) are one of the common neurological diseases, with an incidence of about 5% in the general population (Carpenter et al., 2016). IAs mostly occurred in abnormal bulging on the walls of intracranial arteries, which are the first cause of subarachnoid hemorrhage (SAH). Although SAH occurred at a rate of approximately 1% per year, the consequences are very serious with high rates of mortality (up to 50%) and disability (about 30%) (Nieuwkamp et al., 2009; Chalouhi et al., 2012). Therefore, it is very important to improve the prognosis of SAH patients. It is of great significance to identify the characteristic factors expressed in the blood of SAH patients and give early and active control to reduce the mortality and disability rate of patients.

Immunity plays an important role in the occurrence and development of SAH. Previous studies have reported that immunity plays a role in persistent damage such as cerebral vasospasm after SAH (Mohme et al., 2020; Li et al., 2020). SAH induces peripheral activation of innate immune cells and early brain infiltration. Previous evidence indicated that inflammation is induced following SAH, and immune cells represent a potential therapeutic target, which could help SAH patients in need of new therapies (Gris et al., 2019). For example, Roa et al. (2020) indicated that CD8 and CD161 combined with lymphocytes might be associated with inflammatory response after SAH. Besides, the immune repertoire of T cell receptor (TCR) might help study the mechanism of T cell immunology. Kim et al. (2020) found TCRB and CDR3 repertoires might be regarded as key biomarkers to distinguish SAH patients. Moreover, Zhou et al. (2017) reported that the changes in im-

Received 14 December 2021, accepted 27 June 2022

mune cell subgroups, such as NK, NKT, CD3+, CD4+ and CD8+ were related to clinical prognosis of SAH patients. These factors might be novel biomarkers to evaluate the diagnosis of SAH patients.

Therefore, in our study, we combined SAH with immune cells by integrating multiple SAH expression profile data. We first screen the SAH-related genes. Then, based on the single sample gene set enrichment analysis (ssGSEA) algorithm, we evaluated the immune characteristics of the samples, and compared with the differences of various immune cells in different classification groups. Moreover, we focused on the different immune cell types. Then, the relevant genes are obtained through correlation analysis with these immune cell types, and finally the hub genes related to the SAH were screened through the optimization algorithm.

METHODS

Experimental data and sources

The datasets were searched from National Center for Biotechnology Information database Gene Expression Omnibus (GEO) using the key words of subarachnoid hemorrhage and Homo sapiens (Barrett et al., 2007). The dataset selection criteria were as follows: 1. Blood tissue samples; 2. Different types of samples with diseases and controls; 3. The total number of samples is not less than 50. Subsequently, 2 datasets (GSE73378 (van't Hof et al., 2015) and GSE36791 (Pera et al., 2013)) were obtained from the platform GPL10558 Illumina HumanHT-12 V4.0 expression bead chip that meet these requirements. GSE73378 contained a total of 226 human blood samples, in which we selected 210 samples including 103 SAH patient samples and 107 control samples. And, GSE36791 contained 61 human blood samples which included 43 patient samples and 18 control samples.

Screening of differentially expressed genes

GSE73378 and GSE36791 datasets were obtained from different batches of gene expression level data. The sva package in R3.6.1 (Leek et al., 2012) (version 3.38.0, http://www.bioconductor.org/packages/release/bioc/html/sva.html) was performed to remove the batch effect on the two datasets. And then we obtained the combined expression level data. After that, the limma package in R3.6.1 (Ritchie et al., 2015) (version 3.34.7, https://bioconductor.org/packages/release/bioc/html/limma.html) was used to screen the DERs between the SAH patient samples and the controls with the cut-off of FDR<0.05 and |log2FC|>0.263.

Screening of DERs related to immune cells

The microenvironment is mainly composed of related fibroblasts, immune cells, extracellular matrix, various growth factors, inflammatory factors, and special physical and chemical characteristics. The microenvironment significantly affects the diagnosis of diseases, survival outcomes and clinical treatment sensitivity. Cells in the microenvironment could be clustered into different categories, and there are complex and significant interactions between each type of cell and other cells, and there are some robust cell infiltration patterns. To evaluate the immune cells type of the combined samples, we downloaded the immunologic signature gene sets from Gene Set Enrichment Analysis (GSEA) (Subramanian et al., 2005) (http://software.broadinstitute.org/gsea/index.jsp). Then, the gene set variation analysis for microarray and RNA-Seq data (GSVA) in R3.6.1 (version 1.36.3, http://www.bioconductor.org/packages/release/bioc/html/GSVA.html) was used to evaluate the immune infiltration type of the combined samples. GSVA is called gene set variation analysis, which is a non-parametric unsupervised analysis method, which mainly converts the expression matrix of genes between different samples into the expression matrix of gene sets between samples. GSVA is used to evaluate whether different immune infiltrations are enriched in different samples, using each immune infiltrating cell type as background data. Then we compare the differences in the proportion of individual immune cells between SAH disease and normal control samples.

Screening of DEGs related to immune cells

There were significantly different immune cell types between the screened DEGs and the SAH and the control samples that were evaluated based on ssGSEA method. The cor function in R3.6.1 (http://77.66.12.57/R-help/cor.test.html) was used to calculated Pearson correlation coefficient (PCC) of immune cell types. Subsequently, we only retained the DEGs with the cut-off of P<0.05 as the DEGs significantly associated with immune cells. After that, the analysis of the Gene Ontology (Eguía-Aguilar et al., 2014; Ritchie et al., 2015) biological process, and Kyoto Encyclopedia of Genes and Genomes (KEGG) pathway enrichment annotation, based on the Database for Annotation, Visualization and Integrated Discovery (DAVID) (version 6.8,

https://david.ncifcrf.gov/) (Huang et al., 2009a,b), was performed on the intersecting DEGs with $P<0.05$ as the threshold.

Construction of interaction network and analysis of topology

We searched the interaction relationship between the DEGs related to immune cells and its product protein using the STRING (Szklarczyk et al., 2017) (version 11.0, http://string-db.org/) database. Subsequently, we constructed the interaction network that was visualized through Cytoscape (Shannon et al., 2003) (version 3.6.1, http://www.cytoscape.org/). Besides, the KEGG enrichment annotation analysis based on DAVID (Huang et al., 2009a,b) was performed for the DEGs that constructed interaction network. After that, we searched the KEGG pathway using the keyword of subarachnoid hemorrhage from Comparative Toxicogenomics Database 2019 update (Davis et al., 2019) (http://ctd.mdibl.org/). Then, we compared these KEGG pathways with the KEGG pathways significant related to the genes in interaction network. Finally, we obtained the important overlapping pathways.

Screening and validation of important biomarkers

Least absolute shrinkage and selection operator (LASSO) and recursive feature elimination (RFE) were used to screen the feature genes based on the genes involving the important KEGG pathways. Then, the lars package in R3.6.1 (Usai et al., 2012) (version 1.2, https://cran.r-project.org/web/packages/lars/index.html) was used to perform regression analysis on the target genes to screen the feature genes. After that, RFE method of caret package in R3.6.1 (Deist et al., 2018) (version 6.0-76, https://cran.r-project.org/web/packages/caret) was used to select the optimized feature gene combinations. Then, we selected the overlapping genes as the final feature gene combinations through comparing the results of LASSO and RFE.

To verify the optimized feature genes, we first extract the expression levels of the optimized feature genes from the combined data set and display their expression levels in different groups. Besides, the E-TABM-421 gene expression profile data was downloaded from EBI ArrayExpress (https://www.ebi.ac.uk/), which contained eight samples including four control samples and two SAH samples. After that, we extracted the expression levels of corresponding genes were also extracted from E-TABM-421, and their expression levels in different groups were compared and displayed. In addition, the support vector machine (SVM) method in R3.6.1 e1071 (Wang and Liu, 2015) (version 1.6-8, https://cran.r-project.org/web/packages/e1071) was used to construct disease diagnosis classifier. Then, we evaluated the effectiveness of the model in the combined dataset and E-TABM-421 validation set. The pROC in R 3.6.1 (Robin et al., 2011) (version 1.12.1, https://cran.r-project.org/web/packages/pROC/index.html) was used to calculated the sensitivity (Sen) and specificity (Spe) of ROC.

This study was carried out as shown in Fig. 1.

RESULTS

Screening of DEGs

As shown in Fig. 1A, a total of 530 DEGs were screened between the control and SAH group. Besides, as shown in Fig. 1B, the heatmap indicated that different types of samples could be separated on the basis of the expression values of the screened DEGs. Moreover, the colors of the heatmap were distinct, indicating that the screened DEGs in each group were characteristic of expression.

Screening of DEGs related to immune cells and analysis of GO and KEGG pathways

A total of 28 immune cell types ratio were obtained. After that, we obtained 7 types of immune cells with significant differences between the proportions of various immune cells in the SAH and CTRL groups, including activated CD8 T cell, effector memory CD38 T cell, center memory CD4 T cell, T follicular helper cell, type 2 T helper cell, monocyte, and neutrophil (Fig. 2).

Moreover, 7 differentially expressed immune cells were obtained by ssGSEA. Subsequently, a total of 408 DEGs related to immune cells were obtained with the cutoff of $P<0.05$ and PCC > 0.4. Besides, we obtained 28 GO BPs (such as immune response, cell surface receptor signaling pathway, inflammatory response and positive regulation of B cell proliferation) and 8 KEGG signaling pathways (such as hematopoietic cell lineage and primary immunodeficiency), which were shown in Fig. 3A and Fig. 3B.

Construction of PPI network and analysis of KEGG pathways

We obtained 699 pairs of interaction relationships with the threshold of interaction score > 0.6. Then,

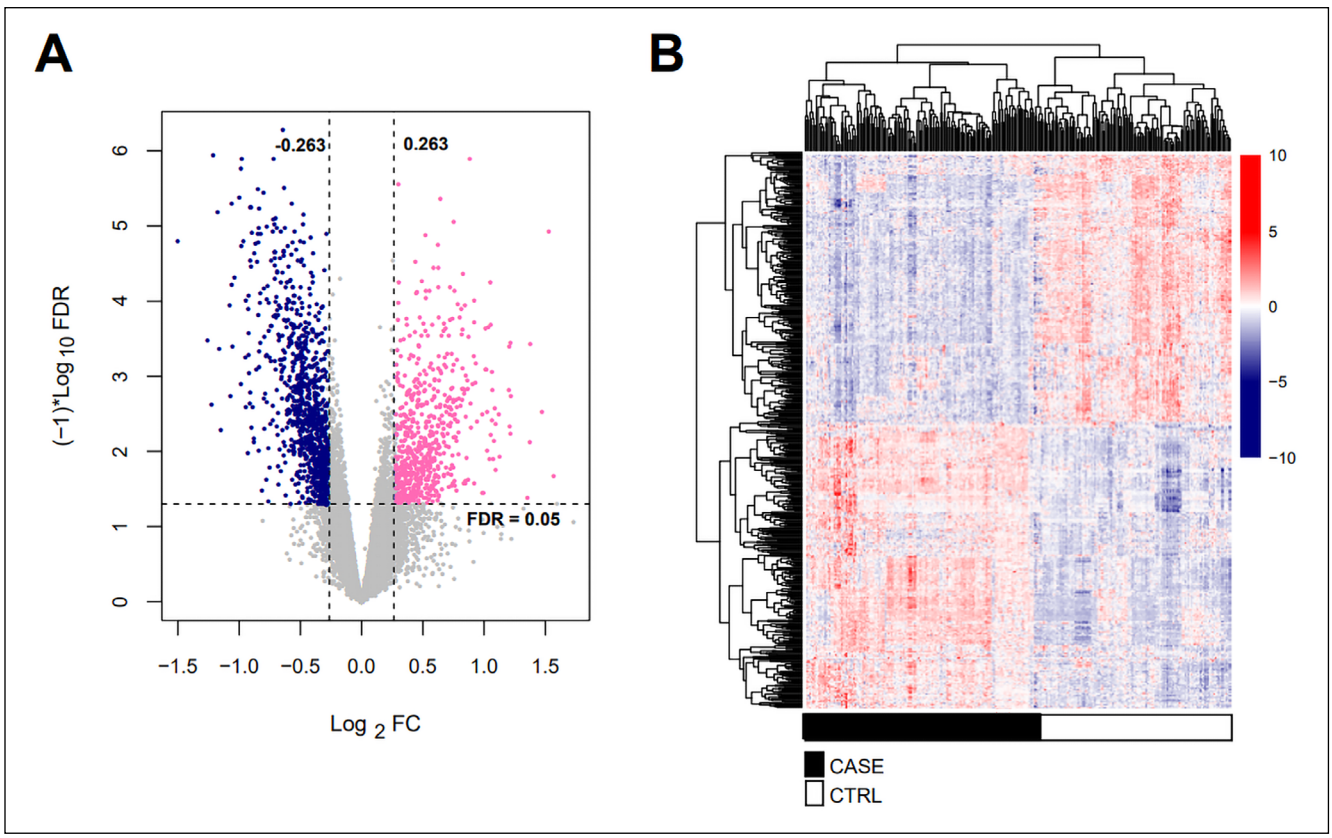

Fig. 1. Screening of DEGs. A indicated the test log_2FC- log_{10}(FDR) of the volcano map. The blue and pink points represent significantly down-regulated and up-regulated DEGs, respectively. The black horizontal line represents FDR<0.05, and the two vertical lines represent |log2FC|>0.263; B indicated the horizontal heat map based on the DEGs expression. The black and white in the sample strip indicated the disease group and the control group, respectively. (DEGs) differentially expressed genes; (FDR) false discovery rate.

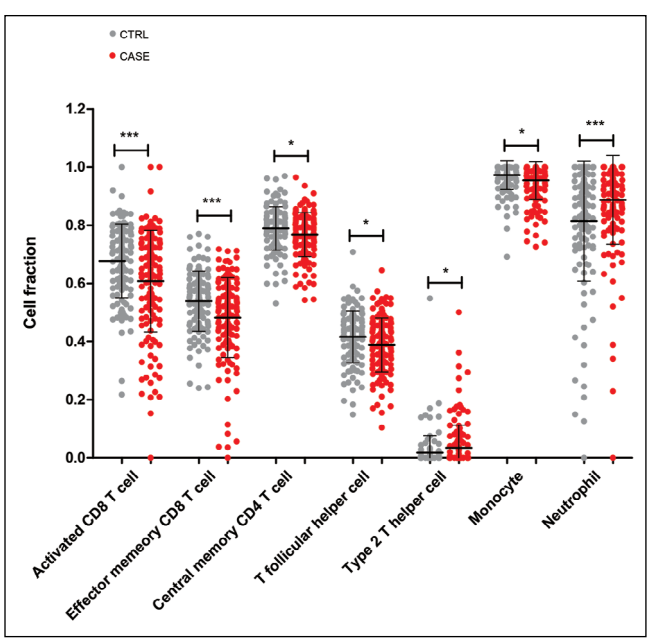

Fig. 2. The distribution map of immune cell types with significant differences between SAH and CTRL groups. (AH) subarachnoid hemorrhage; (CTRL) control.

a PPI network was constructed which included 257 gene nodes, such as *ITGAM*, *MAPK14*, *MMP9*, *GZMB*, *PRF1* and *HDAC1* (Fig. 4). After that, we obtained a total of 14 KEGG pathways. Moreover, we obtained 113 KEGG signaling pathways from CTD database. Subsequently, 10 overlapped KEGG pathways were obtained, which were shown in Table 1. The 10 pathways were hematopoietic cell lineage (including 11 genes, such as *CD2, CD4* and *TGAM*), T cell receptor signaling pathway (including 9 genes, such as *CD4*, *CD8A* and *MAPK14*), NOD-like receptor signaling pathway (including 6 genes, such as *HSP90AB1*, *CASP5* and *CCL5*), Toll-like receptor signaling pathway (including 8 genes, such as *CCL5*, *FOS* and *MAPK14*), natural killer cell mediated cytotoxicity (including 8 genes, such as *GZMB*, *TNFSF10* and *PRF1*), inflammatory mediator regulation of TRP channels (including 7 genes, such as *IL1R1*, *GNAQ* and *MAPK14*), TNF signaling pathway (including 7 genes, such as *CCL5*, *MAPK14* and *MMP9*), leukocyte transendothelial migration (including 7 genes, such as *ITGAM*, *MAPK14* and *MMP9*), cytokine-cytokine receptor interaction (including 11 genes, such as *IL18RAP*, *IL1R1*, *CCL5*) and sphin-

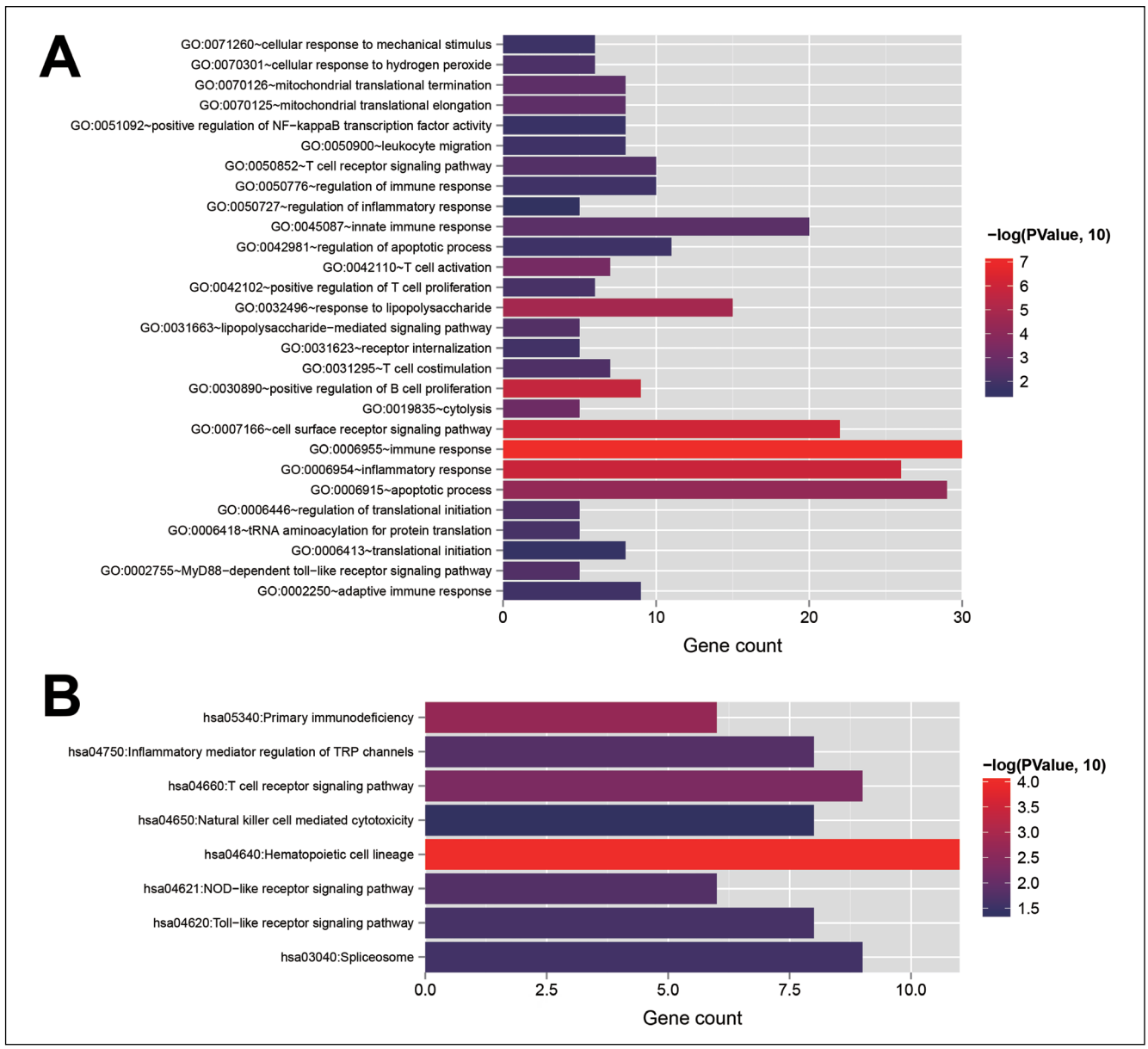

Fig. 3. Analysis of GO and KEGG pathways. The bar graphs of DEGs related to immune cells that involved in biological processes and KEGG signaling pathway. The horizontal axis represented the number of genes, the vertical axis represented the name of the item, the color represents the significance, and the closer the color is to red, the greater the significance. (DEGs) differentially expressed genes; (GO) Gene Ontology; (KEGG) Kyoto Encyclopedia of Genes and Genomes; (SAH) subarachnoid hemorrhage; (CTRL) control.

golipid signaling pathway (including 7 genes, such as *PPP2R2B*, *GNAQ*, *PTEN*), respectively.

Screening and validation of hub genes

A total of 47 DEGs were found that involved in the KEGG pathways related to SAH. Then, 17 and 10 optimized DEGs were screened using LASSO and RFE, respectively. Subsequently, a total of 9 overlapped genes were obtained after comparing the two DEGs combination, including *CCL5*, *CD27*, *CD3D*, *CREB5*, *FYN*, *ITPR3*, *TAB1*, *NCR3* and *S1PR5*, in which, *CCL5*, *FYN*, and *CD3D* were the gene nodes with higher connectivity (Fig. 5A).

It is in the validation data set E-TABM-421 that the expression levels of 9 DEGs are consistent with the direction of expression differences in the combined data set. Among them, CD3D, CREB5, TAB1 and S1PR5 have significant differences (Fig. 5B).

Based on the 9 optimized DEGs, we constructed a sample risk diagnosis model to identify the disease of the sample. We found these DEGs could well help for the diagnosis of SAH (AUC: 0.865) (Fig. 5C). After that, based on the constructed classification diagnosis model, we used the 9 DEGs expression levels in the E-TABM-421 data set to verify the diagnostic model. The result indicated that the 9 DEGs also could apply for identifying disease and evaluate the effect of SAH diagnosis (AUC: 0.750) (Fig. 5D).

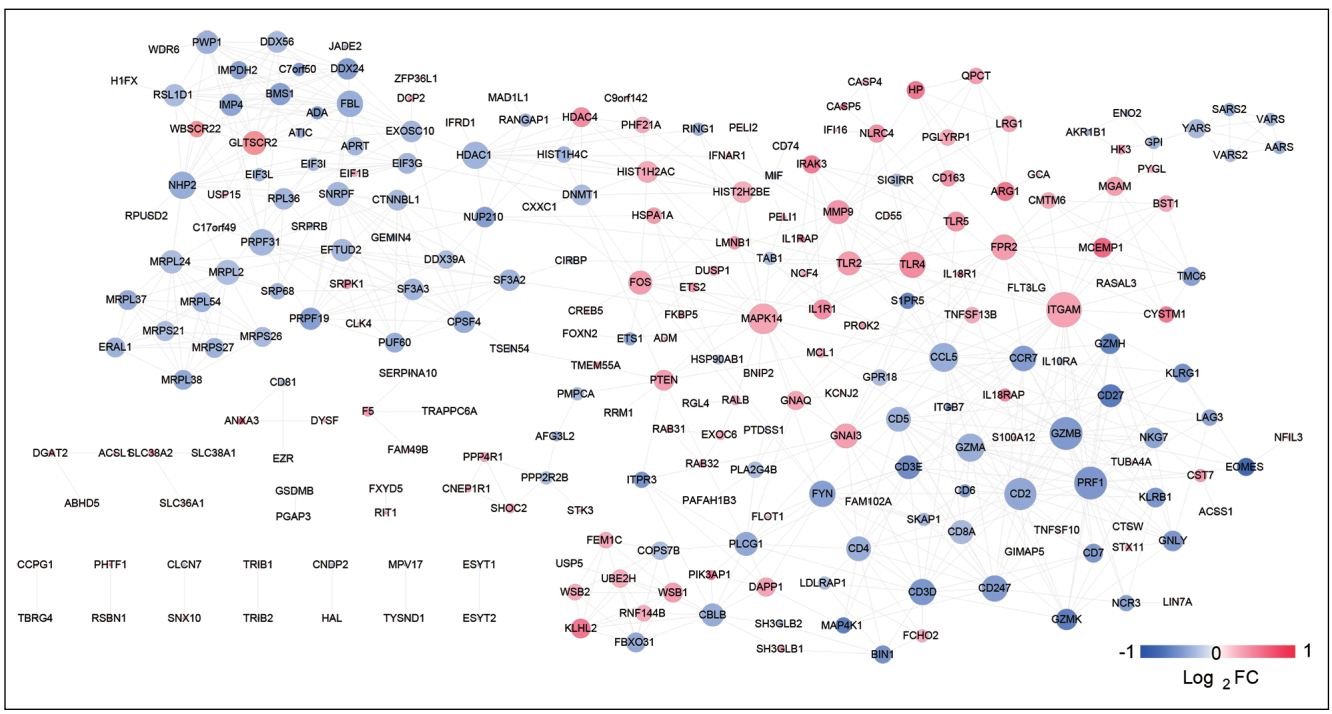

Fig. 4. Construction of PPI network. The change of the color of the node from blue to red indicates the change in the expression of significant difference from significantly down to up, and the size of the node indicates the degree of connectivity of the node in the network. (PPI) protein-protein interaction.

Table 1. 10 overlapped KEGG pathways.

Term	Count	PValue	Genes
*hsa04640: Hematopoietic cell lineage	11	1.92E-05	CD2, CD4, ITGAM
*hsa04660: T cell receptor signaling pathway	9	1.58E-03	CD4, CD8A, MAPK14
*hsa04621: NOD-like receptor signaling pathway	6	7.61E-03	HSP90AB1, CASP5, CCL5
*hsa04620: Toll-like receptor signaling pathway	8	8.80E-03	CCL5, FOS, MAPK14
*hsa04650: Natural killer cell mediated cytotoxicity	8	1.81E-02	GZMB, TNFSF10, PRF1
*hsa04750: Inflammatory mediator regulation of TRP channels	7	2.10E-02	IL1R1, GNAQ, MAPK14
*hsa04668: TNF signaling pathway	7	3.07E-02	CCL5, MAPK14, MMP9
*hsa04670: Leukocyte transendothelial migration	7	4.15E-02	ITGAM, MAPK14, MMP9
*hsa04060: Cytokine-cytokine receptor interaction	11	4.23E-02	IL18RAP, IL1R1, CCL5
*hsa04071: Sphingolipid signaling pathway	7	4.93E-02	PPP2R2B, GNAQ, PTEN

(DEGs) differentially expressed genes; (GO) Gene Ontology, (KEGG) Kyoto Encyclopedia of Genes and Genomes; (PPI) protein-protein interaction.

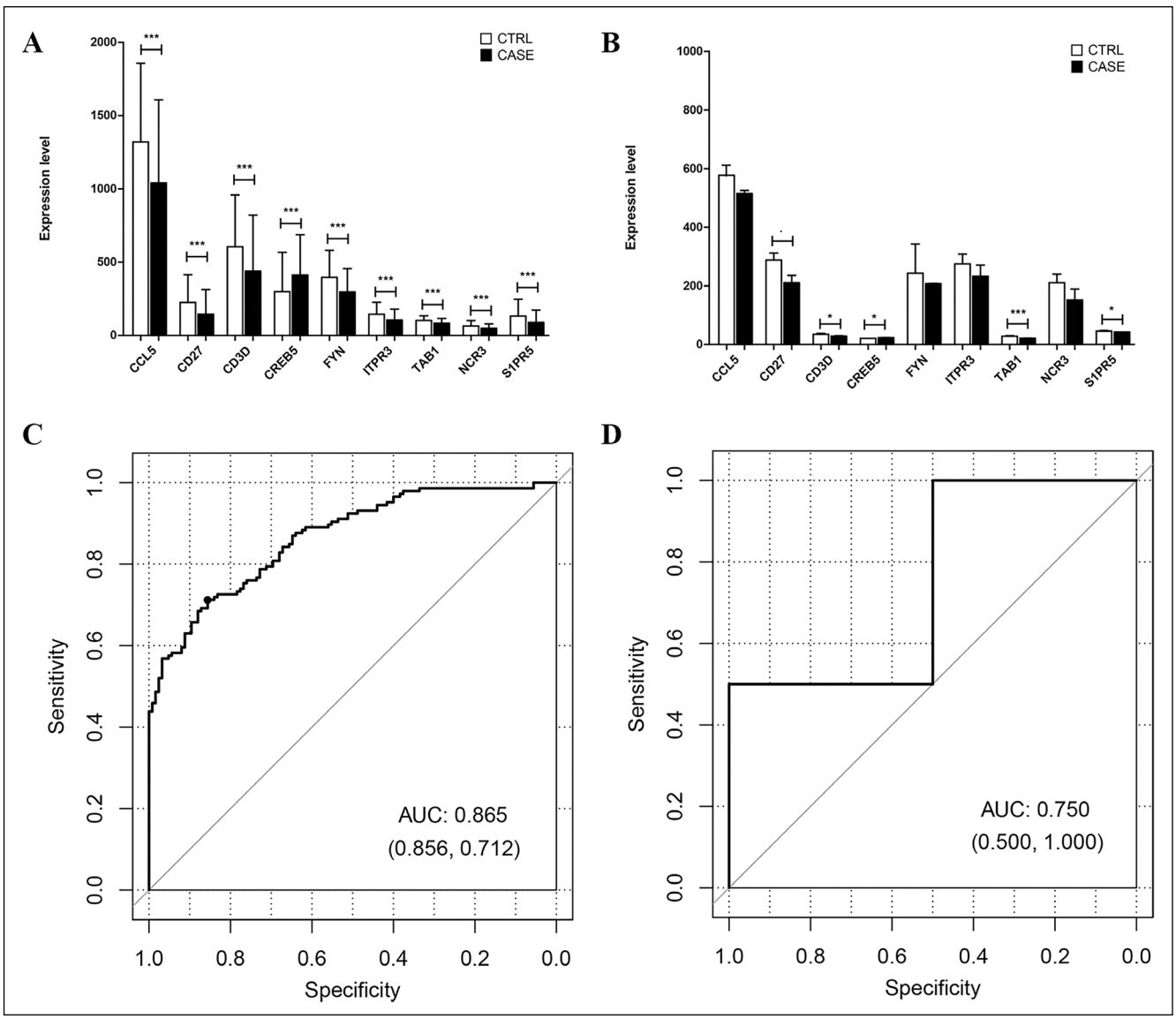

Fig. 5. Screening and validation of hub genes. Combine the 9 optimized DEGs expression levels in the data set (A) and E-TABM-421 (B). * Means *P*<0.05, ** means *P*<0.05, *** means *P*<0.005. Combining the data set (A) and E-TABM-421 (B) based on 9 DEGs sample diagnosis model ROC curve. The numbers in parentheses indicate the Specificity and Sensitivity of the corresponding curve. (DEGs) differentially expressed genes; (ROC) receiver operating characteristic.

DISCUSSION

The immune system changes caused by SAH might affect the prognosis of patients and cause complications (Zhou et al., 2017), which play an important role in SAH. Besides, the finding of biomarkers related to immune cell could help predict the diagnosis of SAH. In our study, we obtained 408 DEGs related to immune cell, based on which we constructed a PPI network. Then, we obtained 10 overlapped KEGG pathways, such as hematopoietic cell lineage, NOD-like receptor signaling pathway and T cell receptor signaling pathway. Subsequently, 9 DEGs related to immune cells (*CCL5*, *CD27*, *CD3D*, *CREB5*, *FYN*, *ITPR3*, *TAB1*, *NCR3* and *S1PR5*) involved in SAH-related KEGG pathways were obtained using LASSO and RFE algorithm. A diagnosis model was successfully constructed based on the 9 DEGs, which could identify the healthy people or SAH patients.

Comparing the KEGG pathways involved in the DEGs with the SAH-related KEGG pathways from CTD dataset, we obtained 10 overlapped immune-related KEGG pathways with significance, among which we found that hematopoietic cell lineage was significantly correlated to SAH. Previous study has indicated that hematopoietic cell lineage pathway might regulate the immune function and participate in the procession of glioblastoma

(Liu et al., 2021). Furthermore, we also found that this pathway was involved in 11 DEGs, such as CD2, CD4 and ITGAM. Among these DEGs, CD4 was reported by previous studies indicating that CD4 might be a biomarker for SAH (Zhao et al., 2019; Pu et al., 2019). The CD4 T cells might have originated from intracisternally injected blood cells and accumulated as a consequence of impaired cerebral lymphatic drainage. Recent reports indicated that lymphatic drainage is crucial for the homeostasis of brain-immune interactions, and its abnormality is involved in the pathogenesis of immune-associated neurological diseases (DeRogatis et al., 2021). Thus, we inferred that CD4 involved in hematopoietic cell lineage pathway might be correlated to neurological deficits following SAH.

SVM is one of the most accurate methods among all well-known data mining algorithms. It is a two-class classification algorithm that can support linear and nonlinear classification. In this study, a SVM classifier was constructed to identify SAH patients. Recent studies have reported that the SVM could identify SAH patients. Danala et al. (2022) constructed a SVM model based on the clinical factor for assessing the diagnosis for SAH with the ROC range from 0.62 ± 0.07 to 0.86 ± 0.07. This result suggested that the SVM model has feasibility to predict diagnosis of SAH patients. In the present study, we also established a SVM model based on 9 immune-related DEGs with ROC of 0.865, indicating that the diagnosis model could also accurately identify SAH patients.

We have constructed a SVM model for distinguishing SAH patients based on 9 DEGs related to immunity. However, this study also has a few limitations. First, we did not elaborate on the detailed pathological mechanisms of these DEGs. In addition, we need to collect a large number of clinical samples to verify whether the SVM model could make diagnosis for SAH. Finally, further experimental studies were needed to verify the functions of these nine key genes.

CONCLUSION

A SVM classifier based on the 9 DEGs (*CCL5*, *CD27*, *CD3D*, *CREB5*, *FYN*, *ITPR3*, *TAB1*, *NCR3* and *S1PR5*) related to immune cells might effectively identify SAH patients or healthy people. Our study might provide a novel method for assessing the diagnosis for SAH.

ACKNOWLEDGEMENT

This work was funded by the Basic Research Program of Jilin Provincial Science and Technology Department (NO. 20150101215JC).

REFERENCES

Barrett T, Troup DB, Wilhite SE, Ledoux P, Rudnev D, Evangelista C, Kim IF, Soboleva A, Tomashevsky M, Edgar R (2007) NCBI GEO: mining tens of millions of expression profiles – database and tools update. Nucleic Acids Res 35: D760–765.

Carpenter CR, Hussain AM, Ward MJ, Zipfel GJ, Fowler S, Pines JM, Sivilotti ML (2016) Spontaneous subarachnoid hemorrhage: a systematic review and meta-analysis describing the diagnostic accuracy of history, physical examination, imaging, and lumbar puncture with an exploration of test thresholds. Acad Emerg Med 23: 963–1003.

Chalouhi N, Ali MS, Jabbour PM, Tjoumakaris SI, Gonzalez LF, Rosenwasser RH, Koch WJ, Dumont AS (2012) Biology of intracranial aneurysms: role of inflammation. J Cereb Blood Flow Metab 32: 1659–1676.

Danala G, Desai M, Ray B, Heidari M, Maryada SKR, Prodan CI, Zheng B (2022) Applying quantitative radiographic image markers to predict clinical complications after aneurysmal subarachnoid hemorrhage: a pilot study. Ann Biomed Eng 50: 413–425.

Davis AP, Grondin CJ, Johnson RJ, Sciaky D, McMorran R, Wiegers J, Wiegers TC, Mattingly CJ (2019) The comparative toxicogenomics database: update 2019. Nucleic Acids Res 47: D948-d954.

Deist TM, Dankers F, Valdes G, Wijsman R, Hsu IC, Oberije C, Lustberg T, van Soest J, Hoebers F, Jochems A, El Naqa I, Wee L, Morin O, Raleigh DR, Bots W, Kaanders JH, Belderbos J, Kwint M, Solberg T, Monshouwer R, Bussink J, Dekker A, Lambin P (2018) Machine learning algorithms for outcome prediction in (chemo)radiotherapy: An empirical comparison of classifiers. Med Phys 45: 3449–3459.

DeRogatis JM, Viramontes KM, Neubert EN, Tinoco R (2021) PSGL-1 immune checkpoint inhibition for CD4(+) T cell cancer immunotherapy. Front Immunol 12: 636238.

Eguía-Aguilar P, Pérezpeña-Díazconti M, Benadón-Darszon E, Chico-Ponce de León F, Gordillo-Domínguez L, Torres-García S, Sadowinski-Pine S, Arenas-Huertero F (2014) Reductions in the expression of miR-124–3p, 330 miR-128–1, and miR-221–3p in pediatric astrocytomas are related to high-grade supratentorial, and recurrent tumors in Mexican children. Childs Nerv Syst 30: 1173–1181.

Gris T, Laplante P, Thebault P, Cayrol R, Najjar A, Joannette-Pilon B, Brillant-Marquis F, Magro E, English SW, Lapointe R, Bojanowski M, Francoeur CL, Cailhier JF (2019) Innate immunity activation in the early brain injury period following subarachnoid hemorrhage. J Neuroinflammation 16: 253.

Huang DW, Sherman BT, Lempicki RA (2009a) Systematic and integrative analysis of large gene lists using DAVID bioinformatics resources. Nat Protoc 4: 44–57.

Huang DW, Sherman BT, Lempicki RA (2009b) Bioinformatics enrichment tools: paths toward the comprehensive functional analysis of large gene lists. Nucleic Acids Res37: 1–13.

Kim BJ, Youn DH, Kim Y, Jeon JP (2020) Characterization of the TCR β chain CDR3 repertoire in subarachnoid hemorrhage patients with delayed cerebral ischemia. Int J Mol Sci 21: 3149.

Leek JT, Johnson WE, Parker HS, Jaffe AE, Storey JD (2012) The sva package for removing batch effects and other unwanted variation in high-throughput experiments. Bioinformatics 28: 882–883.

Li R, Yuan Q, Su Y, Chopp M, Yan T, Chen J (2020) Immune response mediates the cardiac damage after subarachnoid hemorrhage. Exp Neurol 323: 113093.

Liu M, Yu Y, Zhang Z, Chen Z, Chen B, Cheng Y, Wei Y, Li J, Shang H (2021) AEBP1 as a potential immune-related prognostic biomarker in glioblastoma: a bioinformatic analyses. Ann Transl Med 9: 1657.

Mohme M, Sauvigny T, Mader MM, Schweingruber N, Maire CL, Rünger A, Ricklefs F, Regelsberger J, Schmidt NO, Westphal M, Lamszus K, Tolosa E, Czorlich P (2020) Immune characterization in aneurysmal subarachnoid

hemorrhage reveals distinct monocytic activation and chemokine patterns. Transl Stroke Res 11: 1348–1361.

Nieuwkamp DJ, Setz LE, Algra A, Linn FH, de Rooij NK, Rinkel GJ (2009) Changes in case fatality of aneurysmal subarachnoid haemorrhage over time, according to age, sex, and region: a meta-analysis. Lancet Neurol 8: 635–642.

Pera J, Korostynski M, Golda S, Piechota M, Dzbek J, Krzyszkowski T, Dziedzic T, Moskala M, Przewlocki R, Szczudlik A, Slowik A (2013) Gene expression profiling of blood in ruptured intracranial aneurysms: in search of biomarkers. J Cereb Blood Flow Metab 33: 1025–1031.

Pu T, Zou W, Feng W, Zhang Y, Wang L, Wang H, Xiao M (2019) Persistent malfunction of glymphatic and meningeal lymphatic drainage in a mouse model of subarachnoid hemorrhage. Exp Neurobiol 28: 104–118.

Ritchie ME, Phipson B, Wu D, Hu Y, Law CW, Shi W, Smyth GK (2015) Limma powers differential expression analyses for RNA-sequencing and microarray studies. Nucleic Acids Res 43: e47.

Roa JA, Sarkar D, Zanaty M, Ishii D, Lu Y, Karandikar NJ, Hasan DM, Ortega SB, Samaniego EA (2020) Preliminary results in the analysis of the immune response after aneurysmal subarachnoid hemorrhage. Sci Rep 10: 11809.

Robin X, Turck N, Hainard A, Tiberti N, Lisacek F, Sanchez JC, Müller M (2011) pROC: an open-source package for R and S+ to analyze and compare ROC curves. BMC Bioinformatics 12: 77.

Shannon P, Markiel A, Ozier O, Baliga NS, Wang JT, Ramage D, Amin N, Schwikowski B, Ideker T (2003) Cytoscape: a software environment for integrated models of biomolecular interaction networks. Genome Res 13: 2498–2504.

Subramanian A, Tamayo P, Mootha VK, Mukherjee S, Ebert BL, Gillette MA, Paulovich A, Pomeroy SL, Golub TR, Lander ES, Mesirov JP (2005) Gene set enrichment analysis: a knowledge-based approach for interpreting genome-wide expression profiles. Proc Nat Acad Sci 102: 15545–15550.

Szklarczyk D, Morris JH, Cook H, Kuhn M, Wyder S, Simonovic M, Santos A, Doncheva NT, Roth A, Bork P, Jensen LJ, von Mering C (2017) The STRING database in 2017: quality-controlled protein-protein association networks, made broadly accessible. Nucleic Acids Res 45: D362–368.

Usai MG, Carta A, Casu S (2012) Alternative strategies for selecting subsets of predicting SNPs by LASSO-LARS procedure. BMC Proc 6 Suppl 2: S9.

van 't Hof FN, Ruigrok YM, Medic J, Sanjabi B, van der Vlies P, Rinkel GJ, Veldink JH (2015) Whole blood gene expression profiles of patients with a past aneurysmal subarachnoid hemorrhage. PloS One 10: e0139352.

Wang Q, Liu X (2015) Screening of feature genes in distinguishing different types of breast cancer using support vector machine. OncoTargets Ther 8: 2311–2317.

Zhao H, Li ST, Zhu J, Hua XM, Wan L (2019) Analysis of peripheral blood cells' transcriptome in patients with subarachnoid hemorrhage from ruptured aneurysm reveals potential biomarkers. World Neurosurg 129: e16-e22.

Zhou Y, Jiang Y, Peng Y, Zhang M (2017) The quantitative and functional changes of postoperative peripheral blood immune cell subsets relate to prognosis of patients with subarachnoid hemorrhage: a preliminary study. World Neurosurg 108: 206–215.